Polymer 49 (2008) 4546–4551

Contents lists available at ScienceDirect

Polymer

journal homepage: www.elsevier.com/locate/polymer

Water vapor barrier property of organic–silica nanocomposite derived from perhydropolysilazane on polyvinyl alcohol substrate

Reiko Saito*, Takayoshi Hosoya

Department of Organic and Polymeric Materials, Tokyo Institute of Technology, 2-12-1-S1-22, Ookayama, Meguro, Tokyo 152-8552, Japan

ARTICLE INFO

Article history:
Received 11 April 2008
Received in revised form 18 August 2008
Accepted 21 August 2008
Available online 28 August 2008

Keywords:
Nanocomposite
Silica
Water vapor barrier

ABSTRACT

Poly(vinyl alcohol) membrane was coated with organic–silica nanocomposite derived from perhydropolysilazane. For organic composite part, polystyrene-*block*-poly(4-vinyl phenol) [SP], poly(*tert*-butyl acrylate-*co*-2-hydroxyethyl methacrylate) [BA] and poly(butyl methacrylate-*co*-2-hydroxyethyl methacrylate) [BMA] were used. Water vapor barrier property of coat membrane was measured at relative humidity = 96% by a cup method. The coat films of nanocomposites with SP–silica and BA–silica showed better water vapor barrier property than those of the silica coat film without organic polymer and BMA–silica composites. The surface morphologies of the coat films were investigated by scanning electron microscopy and atomic force microscopy. The addition of organic polymer to silica prevented the crack formation of coat layer on the substrate.

1. Introduction

In recent years, poly(vinyl alcohol) (PVA) film has been receiving much attention as an optic and electronic material because of its high transparency and its good gas barrier property against many gases, such as hydrogen, oxygen, nitrogen, etc. [1,2]. On the other hand, due to the high affinity to water, it should be used under very dry condition. For wide application of PVA, the improvement of water vapor barrier property is important.

Various approaches have been developed to increase gas barrier property of polymer films [3]. The formation of organic–inorganic nanocomposite by addition of inorganic compounds, such as montmorillonite, silica, etc., into the organic polymer is convenient and effective approach [4–14]. The inorganic compounds prohibit the permeation of gas through a polymer matrix; therefore, the microscopic and macroscopic dispersions of inorganic compound in the polymer is important to increase the gas barrier property [15,16]. The hybrid of silica with poly(vinyl chloride) drastically decreased water vapor permeability of poly(vinyl chloride) [6]. In the case of poly(urethane), water vapor and oxygen permeabilities decreased by addition of organically modified montmorillonite [8]. In the case of PVA film, the copolymer of ethylene and vinyl alcohol greatly improved the water vapor barrier permeability, however, the barrier properties to other gases were reduced by copolymerization [17,18]. Generally, sol–gel method is a popular and convenient method to provide organic–silica nanocomposites [19–24]. Patil and co-workers synthesized hybrid matrix membrane with PVA–tetraethoxysilane as oxygen barrier, however, water vapor barrier property was not investigated [25].

Gas barrier property of a substrate is greatly improved by coating with good gas barrier materials, such as silica, metal-oxide compounds, etc. [26–30]. For water vapor, silica [31,32], metal-oxide compound [33,34] and organic–silica nanocomposites [35–38] were good coating materials as the barrier films.

The organic–silica nanocomposites were easily formed on the substrates by casting the blend solution of perhydropolysilazane (PHPS, Fig. 1) and organic polymer containing hydroxyl group [39–42]. PHPS is converted to silica under ambient conditions. The surface hardness of organic–silica nanocomposites provided from PHPS was larger than 1.0 GPa [43–45], the coat films were highly transparent [44,45].

The coat film provided with PHPS will be a good water vapor barrier film on the PVA substrate. The morphology of the microphase separation of the composite, which influences the formation of path for water vapor, and the chemical structure of organic polymer are important factors of water vapor barrier property. The morphology of microphase separation of the composite was strongly governed by the architecture of organic polymer and the content of PHPS [44]. In this work, we investigated the effects of organic polymer and silica content of composites on the water vapor barrier property of coat film provided on the PVA substrate. For the coat film, four types of copolymers, polystyrene-*block*-poly(4-vinyl phenol) (SP), poly(*tert*-butyl acrylate-*co*-2-hydroxyethyl methacrylate (HEMA)) (BA) and poly(butyl methacrylate-*co*-HEMA) (BMA) were used. The water vapor permeability coefficient, *Q*, was measured by a cup method.

* Corresponding author. Tel./fax: +81 3 5734 2937.
E-mail address: rsaito@polymer.titech.ac.jp (R. Saito).

0032-3861/$ – see front matter © 2008 Elsevier Ltd. All rights reserved.
doi:10.1016/j.polymer.2008.08.040

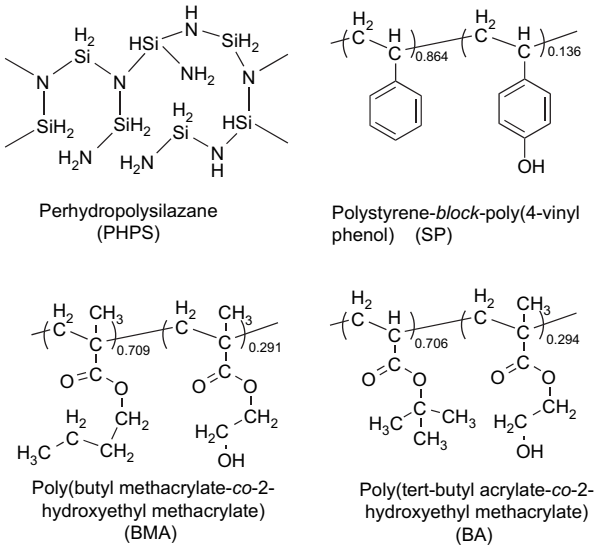

Fig. 1. Chemical structures of perhydropolysilazane (PHPS), polystyrene-*block*-poly (4-vinyl phenol), poly(butyl methacrylate-*co*-2-hydroxyethyl methacrylate) and poly (*tert*-butyl acrylate-*co*-2-hydroxyethyl methacrylate).

2. Experimental

2.1. Materials

tert-Butyl acrylate (Tokyo Chemical Industry, 99.0%), HEMA (Tokyo Chemical Industry, 95.0%), butyl methacrylate (Kanto Chemical, 98%) were purified by distillation under vacuum. Toluene (Kanto Chemical, 99.0%) was dried over calcium hydride (Kanto Chemical,>95.0%) for 24 h, and distilled under vacuum. PHPS/xylene solution (NN-110, AZ electronic materials, 20 wt% of PHPS), PVA (Kanto Chemical, M_n: 22,000), *N*,*N*′-azobisisobutyronitrile (AIBN, Kanto Chemical, 97.0%), 2-butanone (Kanto Chemical, 99.0%), *n*-hexane (Kanto Chemical, 99.0%), tetrahydrofuran (THF, Kanto Chemical, 99.5%), acetic anhydride (Kanto Chemical, 97.0%), phosphorus(V) oxide (Kanto Chemical, 97.5%), chloroform-*d* (Kanto Chemical, 98.0%)and ammonium nitrate (Kanto Chemical, 98.5%) were used as-received. Polystyrene-*block*-poly(4-vinyl phenol) (SP) was previously synthesized and characterized elsewhere [43].

2.2. Synthesis of poly(tert-butyl acrylate-co-2-hydroxyethyl methacrylate) (BA) and poly(butyl methacrylate-co-2-hydroxyethyl methacrylate) (BMA)

tert-Butyl acrylate or butyl methacrylate (10 mL), HEMA (2.0 mL), AIBN (0.060 g) and 2-butanone (10 mL) were added to a sealable Pyrex flask. The flask was sealed under vacuum, and heated at 60 °C for 3.0 h. After the reaction, the solution was cooled to room temperature and poured into *n*-hexane (100 mL). Precipitated polymer was collected by filtration and purified for three times by re-precipitation with 2-butanone (10 mL) and *n*-hexane (50 mL). Then, polymer was freeze-dried under vacuum. Number-average molecular weight ($\overline{M}_n$) and molecular weight distribution ($\overline{M}_w/\overline{M}_n$) were determined by Gel Permeation Chromatography (GPC). Content of HEMA was determined by proton nuclear magnetic resonance (^{1}H NMR) spectrometry.

2.3. Preparation of coat film

PVA film (55 mm × 65 mm, average thickness: 52.6 ± 10 μm) was prepared on poly(propylene) film (Sumitomo-3M, PP2500) by casting PVA water solution (PVA concentration:12 wt%) and dried at room temperature for 3 days and under vacuum for 24 h. To prepare coat solution, polymer (0.097 g) was dissolved in toluene (9.7 mL). NN-110 (0.84 mL) was gradually added to the polymer solution under nitrogen and stirred for 24 h at room temperature. The coat solution (1 mL) was cast on the PVA substrate and dried at room temperature for a day.

2.4. Characterization

GPC was performed using a gel permeation chromatograph (HITACHI, L-7000) detected with refractive index spectrometer (HITACHI, L-2490), column TSKgel-G5000H_{HR} (the optimum range of M_w: $<4\times10^6$ in THF). Eluent, flow-rate and temperature were THF, 0.6 mL min^{-1} and 35 °C. $\overline{M}_n$ was calibrated with standard PMMA. ^{1}H NMR measurement was carried out with ^{1}H NMR spectrometer (JEOL, GSX-400 Hz) with deuterated chloroform (chloroform-*d*) as a solvent at room temperature using the signal of the deuterated solvent as lock and the internal standard for chemical shift data in the δ-scale relative to tetramethylsilane. For differential scanning calorimetric measurement, 10 mg of polymer was sealed in an aluminum pan and measured with a differential scanning calorimeter (Perkin–Elmer, Pyris 1) in a temperature range of −50 to 150 °C with ramping rate 20 K min^{-1}. The morphology of the fractured surfaces was investigated using an S-800 (Hitachi, Japan) scanning electron microscope operated with 1.0 kV, and an SPA300 (Seko Instruments, Japan) atomic force microscopy in air in tapping mode with silicon cantilever (OMCL-TR400PSA-1, Olympus).

2.5. Measurement of water vapor permeability

Each specimen was sealed with silicon past (Sin-Etsu Silicon, KE45W) on Pyrex glass cups containing 2.0 g of phosphorus(V) oxide. The cups were 30 mm (inner diameter), 32 mm (outer diameter) and 13 mm (depth) with an exposure film area of 706.5 mm^2. The test cups were placed in an air-tight plastic desiccator containing 20 mL of distilled water (96 ± 2% of Relative Humidity (RH)) at 23 ± 2 °C. The cups were weighted to the nearest 0.1 mg for 24 h intervals for 4 days. Regression analysis of weight increase as a function of time was performed to insure that accurate steady state slopes were obtained. Water vapor permeability coefficient of whole film (Q_{total}) was calculated by the following equation

$$Q_{total} = \frac{\Delta W l_{total}}{\Delta p S} \quad (1)$$

where ΔW is average weight increase per day, Δp is vapor pressure drop across the film, l_{total} is the film thickness of whole film and S is the exposed film area (706.5 mm^2).

3. Results and discussion

3.1. Characteristics of organic polymer

Characteristics of polymers, polystyrene-*block*-poly(4-vinyl phenol) (SP), poly(butyl methacrylate-*co*-HEMA) (BMA), and poly (*tert*-butyl acrylate-*co*-HEMA) (BA) are listed in Table 1. The content of HEMA or vinyl phenol was set to be less than 30 mol%. Because increasing the hydroxyl group content decreased the solubility of copolymer in hydrophobic solvents that were good solvent for PHPS. Glass transition temperature (T_g) of poly(styrene-*co*-vinyl phenol) with 40 mol% of vinyl phenol was 140.5 °C [46], it was higher than the measurement temperature of water vapor permeability. T_g of poly(butyl methacrylate), 20.0 °C [47], is close to the measurement temperature. The lower T_g of polymer than measurement temperature increases the gas permeability. Thus, T_g of BMA and BA was measured by differential scanning calorimetry. The T_g values, 29.9 °C

Table 1
Characteristics of organic polymers for coating

Code	Polymer type	Content of HEMA or vinyl phenol[a] (mol%)	$\overline{M}_n$[b]	$\overline{M}_w/\overline{M}_n$[b]	T_g[c] (°C)
SP	Polystyrene-*block*-poly (4-vinyl phenol)	13.6	1.45×10^5	1.40	–
BMA	Poly(butyl methacrylate-*co*-2-hydroxyethyl methacrylate)	29.1	1.36×10^5	2.35	29.9
BA	Poly(*tert*-butyl acrylate-*co*-2-hydroxyethyl methacrylate	29.4	2.40×10^5	2.36	30.4

[a] Determined by ^{1}H NMR.
[b] Determined by GPC with calibration of poly(methyl methacrylate) standards.
[c] Determined by DSC.

for BMA and 30.4 °C for BA, were higher than the measurement temperature; BMA and BA were suitable for coating.

3.2. Preparation of poly(vinyl alcohol) substrate and coated films

First, the PVA substrates were prepared by casting on PET sheet. Then, the coat solutions were cast on the substrates and dried gradually. To provide silica domains, PHPS solution was used. In the case of PHPS thin film, PHPS was completely converted to silica for 6 h [48]. In the case of blend film of PHPS and organic polymer containing hydroxyl group, PHPS was gradually and completely converted to silica at room temperature after drying [41]. It took about 8 h to dry the film completely. For complete conversion of silica, the coat films were dried at room temperature for 24 h in this work. In the case of the coating with organic–silica composites, PHPS and organic polymer were reacted in solution for 24 h before coating. It was already reported that the reaction of PHPS and hydroxyl group of organic polymer immediately proceeded, and completed by 8 h [40]. Therefore, the grafting of PHPS onto organic polymer was completed in the coat solution. After coating, the coated PVA substrates were transparent, and the composite layers were well sticked on the substrate.

3.3. Water vapor permeability of the PVA substrate and the coat films

Water vapor permeability of the films at relative humidity (RH) = 96 ± 2% was measured by the cup method. The water vapor permeability constant of whole film (Q_{total}) was calculated by using Eq. (1) with the increase weight of cap in the range of 24–96 h, in which permeation rate was constant. Water vapor permeability (Q_{total}) and thickness of film (l_{total}) of the whole film are listed in Table 2. First, water vapor barrier property of poly(vinyl alcohol) (PVA) substrate was investigated. When the PVA substrate was not coated, water vapor permeability coefficient of PVA substrate (Q_{PVA}) equals to Q_{total}. The Q_{PVA} was 752.6 g μm m^{-2} day^{-1} mmHg^{-1}, and well agreed with the literature [2].

Next, the effect of coating was investigated. Except for BMA1, the Q_{total} values decreased by coating, water vapor barrier property of the PVA substrate was improved by coating in this work. In order to clarify the water vapor barrier property of coat layer, the water vapor permeability of coat layer was determined. In the case of multi-layered film, gas pressure decreases at each layer. The whole gas permeability of multi-layered film with n layers, Q_{total}, is given by [49]

$$l_{total}/Q_{total} = \sum_{i=1}^{n}(l_i/Q_i) \quad (2)$$

where l_{total} is the whole film thickness, l_i and Q_i are the thickness and gas permeability of layer i, respectively. In this work, the coated film was composed of the PVA substrate and the coat layer. Eq. (2) becomes

$$l_{total}/Q_{total} = l_{PVA}/Q_{PVA} + l_{coat}/Q_{coat} \quad (3)$$

where Q_{coat} is the water vapor permeability of coat layer, l_{coat} is an

Table 2
Content of coat film and water vapor permeability coefficients

Code	Polymer for composite layer[a]	Silica content in composite layer (vol%)	Thickness (μm)			Water vapor pressure (mmHg)	Q_{total} (g μm m^{-2} day^{-1} mmHg^{-1})	Q_{coat} (g μm m^{-2} day^{-1} mmHg^{-1})	Q_{total}/Q_{PVA}	Q_{coat}/Q_{PVA}
			Whole film	PVA	Coat layer					
PVA	None	0.0	42.2	42.4	0.0	13.93	752.6	0.00	1.00	0.00
PHPS1	Silica	100.0	83.5	81.4	2.10	16.34	520.7	129.9	0.69	0.173
PHPS2	Silica	100.0	41.6	33.2	8.40	17.02	332.4	92.74	0.44	0.123
SP1	SP	0.0	66.3	59.8	6.45	18.69	336.0	55.83	0.45	0.074
SP2	SP	18.5	70.4	66.8	3.60	18.69	403.3	65.72	0.54	0.087
SP3	SP	31.8	41.1	38.0	3.10	17.20	247.0	34.54	0.33	0.046
SP4	SP	41.2	57.0	52.6	4.40	17.20	268.5	40.14	0.36	0.053
BMA1	BMA	0.0	72.0	67.0	5.00	17.15	766.2	1234.7	1.02	1.641
BMA2	BMA	29.7	69.5	61.0	8.50	17.15	488.9	111.73	0.65	0.148
BMA3	BMA	45.8	70.9	65.2	5.70	17.15	644.8	288.66	0.86	0.384
BMA4	BMA	55.0	58.1	52.4	5.70	17.15	670.0	204.85	0.89	0.272
BA1	BA	0.0	66.3	59.8	6.33	13.50	388.3	49.43	0.52	0.066
BA2	BA	55.2	67.6	65.4	2.32	13.50	355.7	34.89	0.47	0.046
BA3	BA	64.9	52.2	49.5	2.66	13.50	401.7	35.75	0.53	0.047
BA4	BA	71.1	62.7	57.0	5.74	16.55	384.3	56.71	0.51	0.074
BA5	BA	81.1	70.0	64.2	5.80	16.55	364.2	57.96	0.48	0.077

Relative humidity = 96 ± 2%. Temperature = 22 °C.
[a] SP: polystyrene-*block*-poly(4-vinyl phenol). BMA: poly(butyl methacrylate-*co*-2-hydroxyethyl methacrylate). BA: poly(*tert*-butyl acrylate-*co*-2-hydroxethyl methacrylate).

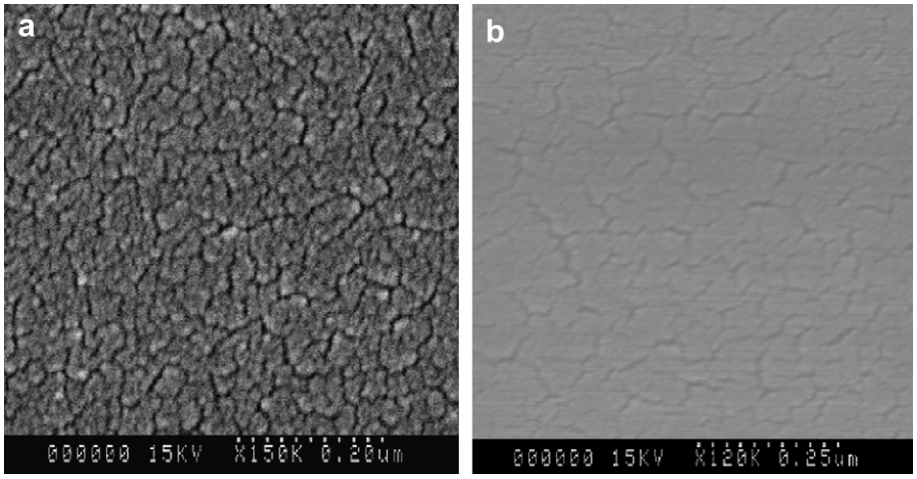

Fig. 2. SEM images of surface of coat films on PVA substrate. (a) PHPS1 and (b) PHPS2.

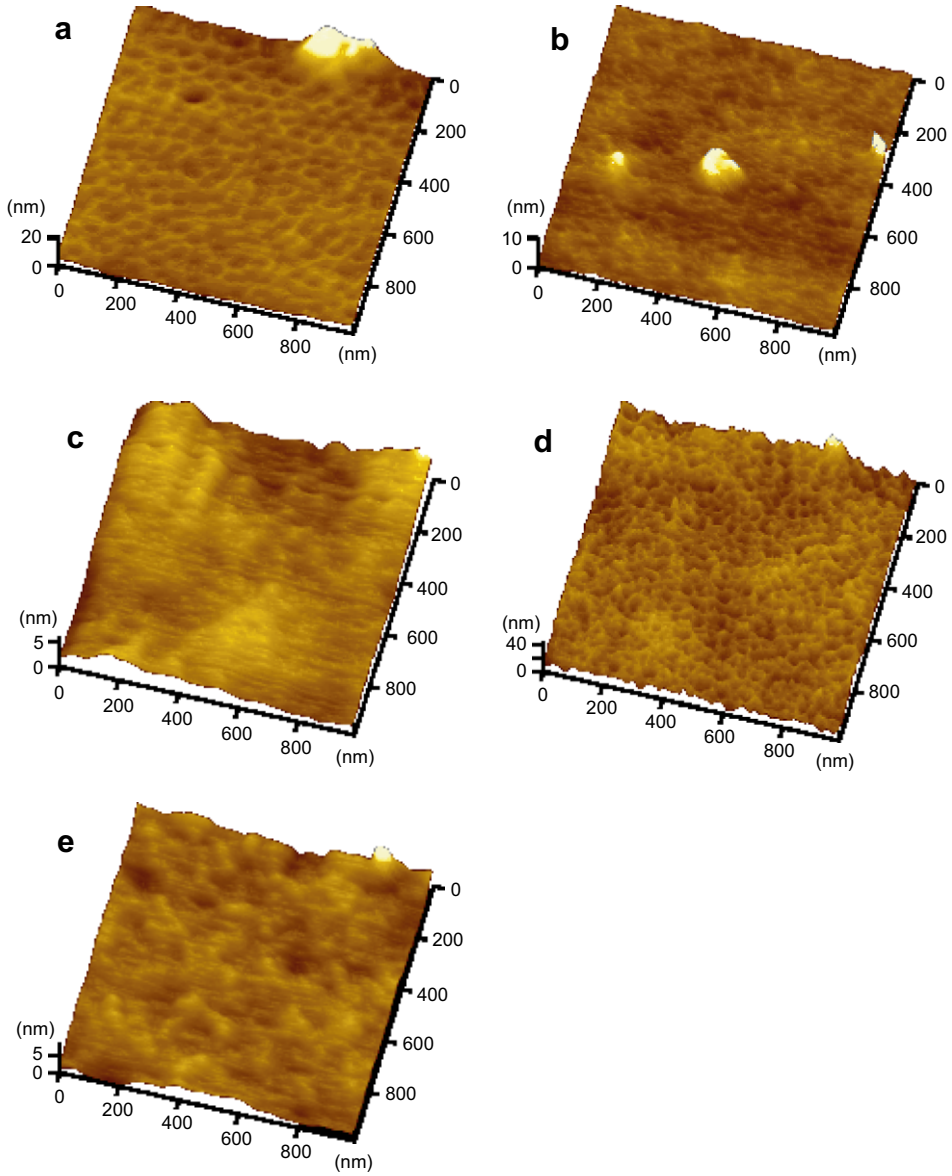

Fig. 3. AFM images of surface of coat films on PVA substrate. (a) SP1 with SP, (b) BMA1 with BMA, (c) BA1 with BA, (d) SP3, the composite of SP with 31.8 vol% of silica, and (e) BA2, the composite of BA with 55.2 vol% of silica.

average thickness of coat layer calculated from l_{total} and l_{PVA}. The water vapor permeability of coat layer, Q_{coat}, was calculated from Q_{total} by Eq. (3). Table 2 lists Q_{coat}, Q_{total}/Q_{PVA} and Q_{coat}/Q_{PVA}.

When the substrate was coated with silica provided from perhydropolysilazane (PHPS)/xylene mixture, Q_{coat} of PHPS2 was smaller than that of PHPS1. Theoretically, Q_{coat} does not depend on the thickness of coat layer. The improvement of water vapor barrier property by increasing the thickness of silica layer was due to the prevention of crack formation in the coat layer. This will be discussed in later section.

In the case of BMA series, the water vapor barrier property was insufficiently improved. Q_{coat} of BMA1 was larger than Q_{PVA}. The gas barrier property of organic polymer was determined by the excluded volume of monomer units and its packing state. The large exclusion volume of *n*-butyl group of BMA would cause the large permeability of water vapor. Because of the blocking of water vapor by silica domain in BMA, the water vapor permeability of the composites (BMA2–4) was slightly reduced. However, their permeability was still higher than that of PHPS2.

In the cases of SP series and BA series, their Q_{coat} values were apparently lower than that of PHPS2 (92.74 g μm m^{-2} day^{-1} $mmHg^{-1}$). The Q_{coat} values of SP1 and BA1 were about the half of that of PHPS2. The addition of silica to PS or BA enhanced the water vapor barrier property of the coat layer. The Q_{coat}/Q_{PVA} values of the composites of SP and BA were lower than that of SP1 and BA1, the path of water vapor in the organic polymers, SP and BA, would be blocked with silica domains by forming nanocomposite. In the case of SP series, the Q_{coat}/Q_{PVA} sensitively depended on the silica content. The minimum Q_{coat}/Q_{PVA} (0.046) was observed at 31.8 vol% of silica content (SP3). To compare with SP series, less influence of silica content for BA series was considered. It may be due to the architectures of BA and SP. The region of minimum Q_{coat}/Q_{PVA} of BA series was observed in the region of 55.2 from 64.9 vol% of silica content (BA2 and BA3). For both SP and BA series, the minimum values were very similar. It was concluded that SP and BA were suitable polymers for coating PVA substrate.

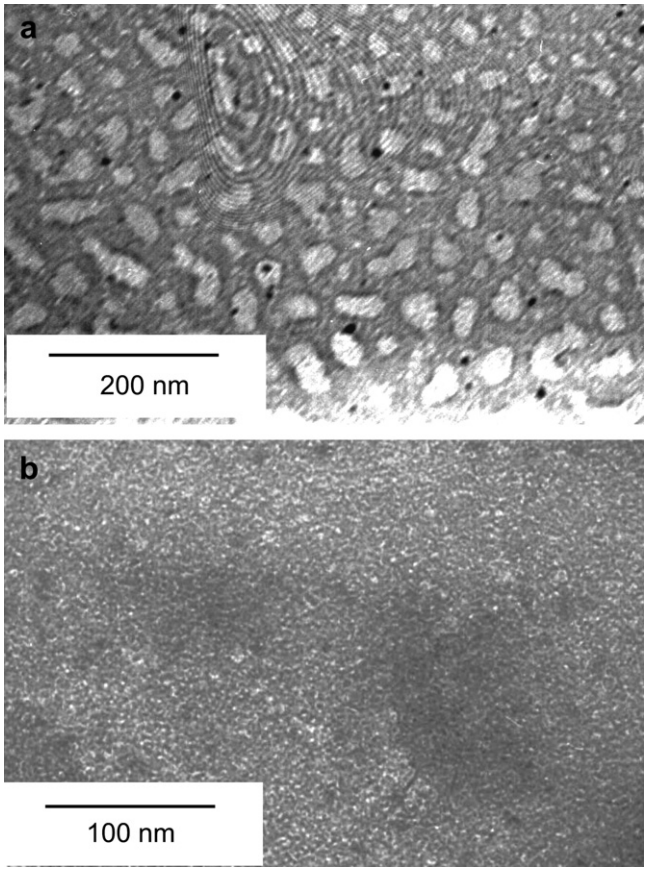

Fig. 4. TEM images of as-cast film of coat solution. (a) SP3, the composite of SP with 31.8 vol% of silica content [43], and (b) BA2, the composite of BA with 55.2 vol% of silica content.

3.4. Morphological observation of coat films

To investigate the effect of morphology of the coat film, the surface of the coat films was observed by Scanning Electron Microscopy (SEM) and Atomic Force Microscopy (AFM). Fig. 2 shows the SEM micrographs of the surface of PHPS1 and PHPS2. Due to 68 vol% of shrinkage of PHPS layer by conversion to silica [39], many deep cracks, which act as the path for the water vapor, were formed on the surface of PHPS1. The cracks reduced by increasing the thickness of silica layer (PHPS2), because of the increasing of toughness of silica layer. Thus, the water vapor barrier property of coat layer was enhanced by increasing the thickness of silica layer. However, the cracks were not completely removed from PHPS2, Q_{coat} of PHPS2 was still larger than those of coat films of SP and BA series.

Fig. 3 shows the typical AFM images of the surface. For all cases, the surface was completely covered with coat layer, the high water vapor permeability of BMA1 was due to the chemical structure of BMA. In the case of SP1 (Fig. 3a), taking account of the architecture of SP, the crater-like structure corresponds to polystyrene-rich domains. The depth of craters was in the range from 5 to 18 nm. In the cases of the composites of SP3 and BA2, the cracks, which were observed for PHPS series, were not observed. This indicates that the stress in the silica domain owing to the calcinations was released by the organic polymers in the composite. For SP3, the addition of silica reduced the size of crater-like structure (Fig. 3d). The morphology of SP3 observed by AFM agreed well with the TEM morphology of the as-cast film of SP3 observed elsewhere [43]. The morphology of microphase separation of as-cast film of SP3 observed by TEM was isolated polystyrene domains in a silica-rich matrix (Fig. 4a) [43]. The average size of crater-like domains (63 nm) agreed well with the average diameter of polystyrene domains observed by TEM. The thickness of wall-like domains observed by AFM (38 nm) showed good agreement with the average distance between polystyrene domains observed by TEM. The wall-like domains on the AFM micrograph were the silica-rich regions, and the crater-like domains were the polystyrene-rich domains. Because of high incompatibility between PHPS and 4-vinyl phenol, the microphase separation was induced between 4-vinyl phenol and PHPS in SP3. In contrast, in SP1, the microphase separation occurred between polystyrene sequence with DP = 1180 and poly(4-vinyl phenol) with DP = 186. Thus, the size of crater-like structure of SP3 was smaller than that of SP1.

In the case of BA2 (Fig. 3e), the average DP of poly(*tert*-butyl acrylate) sequence between HEMA units was only 2.4. The microphase separation of nanocomposite was too small to observe by AFM. Thus, as-cast film of BA2 on carbon substrate was observed by TEM (Fig. 4b). The dark regions correspond to the silica-rich domains. The poly(*tert*-butyl acrylate)–silica lamellar like structure with 3.8 nm in average domain spacing was observed. The Q_{coat}/Q_{PVA} of BA1 was smaller than that of SP1. The water vapor barrier property of BA was slightly better than that of SP. However, the similar water vapor barrier property was observed for BA2 with 55.2 vol% of silica and SP3 with 31.8 vol% of silica. The minimum Q_{coat}/Q_{PVA} was achieved with less silica content for SP. It would be due to the fine control of microphase separation with block copolymer. In contrast, the most important advantage of BA was easy production by conventional radical polymerization. In conclusion, not only block copolymer with well-controlled architecture but also random copolymer was useful to form the organic–silica nanocomposite for water vapor barrier film.

4. Conclusion

In order to increase the water vapor barrier property of the PVA substrate, silica or organic–silica nanocomposites provided from PHPS were cast on the PVA substrate. When the substrate was coated with silica, cracks were formed on the silica layer. The increase of the thickness of silica layer reduced the crack formation, and the water vapor barrier property was slightly improved. It was considered that the toughness of silica layer increases by increasing the thickness of coat layer. The order to water vapor barrier property of organic polymers was BA > SP > BMA. The low water vapor barrier property of BMA would be due to the bulky butyl group in the poly(butyl methacrylate) sequence. For all coat polymers, the hybrid of silica by grafting PHPS onto the organic polymers reduced the water vapor permeability constant. The optimum microphase separation of organic–silica nanocomposite for the water vapor barrier property depended on the architectures of organic polymer. Due to the small size of microphase separation, random copolymer BA was effective to improve the water vapor barrier property as well as block copolymer SP.

References

[1] Moroi H. Br Polym J 1998;20(4):335–43.
[2] Cozmuta I, Blanco M, Goddard III WA. J Phys Chem B 2007;111(12):3151–66.
[3] Ward WJ, Gaines Jr GL, Alger MM, Stanley TJ. J Membr Sci 1991;55(1–2):173–80.
[4] Kojima Y, Fukumori K, Usuki A, Okada A, Kurauchi T. J Mater Sci Lett 1993;23(12):889–90.
[5] Yano Z, Usuki A, Okada A, Kurauchi T, Kamigaito O. J Polym Sci Part A Polym Chem 1993;31(10):2493–8.
[6] Ultan S, Balkose D. J Membr Sci 1996;115(2):217–24.
[7] Chang JH, Park DK, Ihn KJ. J Appl Polym Sci 2002;84(12):2294–301.
[8] Osman MA, Mittal V, Morbidelli M, Suter UW. Macromolecules 2003;36(26):9851–8.
[9] Gain O, Espuche E, Pollet E, Alexander M, Dubois PH. J Polym Sci Part B Polym Phys 2005;43(2):205–14.
[10] Jacquwlot E, Espuche E, Gerard JF, Duchet J, Mazabraud P. J Polym Sci Part B Polym Phys 2006;44(2):431–40.
[11] Mazarenko S, Meneghetti P, Julmon P, Olson BG, Qutubuddin S. J Polym Sci Part B Polym Phys 2007;45(13):1733–53.
[12] Mittal V. Eur Polym J 2007;43(9):3727–36.
[13] Osman MA, Mittal V, Suter UW. Macromol Chem Phys 2007;208(1):68–75.
[14] Ammala A, Pas SJ, Lawrence KA, Stark R, Webb RI, Hill AJ. J Mater Sci 2008;18(8):911–6.
[15] Osman MA, Mittal V, Lusti HR. Macromol Rapid Commun 2004;25(12):1145–9.
[16] Solovyov SE. J Phys Chem B 2006;110(36):17977–86.
[17] Samios CK, Kalfoglou NK. Polymer 1998;39(16):3863–70.
[18] Ito K, Saito Y, Yamamoto T, Ujihira Y, Nomura K. Macromolecules 2001;34(18):6153–5.
[19] Pomogailo AD. Colloid J 2005;67(6):658–77.
[20] Start PR, Mauritz KA. J Polym Sci Part B Polym Phys 2003;41(13):1563–71.
[21] Iwamura T, Adachi K, Chujo Y. Polym J 2004;36(11):871–7.
[22] Ogoshi T, Chujo Y. Compos Interfaces 2005;11(8–9):539–66.
[23] Ogoshi T, Chujo Y. J Polym Sci Part A Polym Chem 2005;43(16):3543–50.
[24] Tamaki R, Naka K, Chujo Y. Polym J 1998;30(1):60–5.
[25] Patil MB, Patil SA, Veerapur RS, Aminabhavi TM. J Appl Polym Sci 2007;104(1):273–8.
[26] Tsubone D, Kodama H, Hasebe T, Hotta A. Surf Coat Technol 2007;201(14):6431–6.
[27] Abbas GA, papakonstantinou P, Okpaluga TIT, McLaughlin JA, Filik J, Harkin-Jones E. Thin Solid Films 2005;482(1–2):201–6.
[28] Vaswuez-Borucki S, Jacob W, Achete CA. Diamond Relat Mater 2000;9(12):1971–8.
[29] Rochat G, Leterrier Y, Fayet P, Manson JAE. Thin Solid Films 2005;484(1–2):94–9.
[30] Roberts AP, Henry BM, Sutton AP, Grovenor CRM, Briggs GAD, Miyamoto T, et al. J Membr Sci 2002;208(1–2):75–88.
[31] Erlat AG, Spontak RJ, Clarke RP, Robinson TC, Haaland PD, Tropsha Y, et al. J Phys Chem B 1999;103(29):6047–55.
[32] Howells DG, Henry BM, Madocks J, Assender HE. Thin Solid Films 2008;516(10):3081–8.
[33] Erlat AG, Henry BM, Ingram JJ, Mountain DB, McGuigan A, Howson RP, et al. Thin Solid Films 2001;338(1–2):78–86.
[34] Ohishi T. J Non-Cryst Solids 2003;332(1): 87–92.
[35] Brown RA, Budd PM, Price C, Satgurunathan R. Eur Polym J 1993;29(2–3):337–42.
[36] Ogino A, Nagatsu M. Thin Solid Films 2007;515(7–8):3597–601.
[37] Takahashi S, Goldberg HA, Feeney CA, Karim DP, Farrell M, O'Leary K, et al. Polymer 2006;47(9):3083–93.
[38] Singh B, Bouchet J, Leterrier Y, Manson JAE, Rocheat G, Fayet P. Surf Coat Technol 2007;202(2):208–16.
[39] Saito R, Kowano K, Tobe T. J Macromol Sci Pure Appl Chem 2002;A39(3):171–82.
[40] Saito R, Mori Y. J Macromol Sci Pure Appl Chem 2002;A39(9):915–34.
[41] Saito R, Tobe T. J Appl Polym Sci 2004;93(2):749–57.
[42] Saito R. J Polym Sci Part A Polym Chem 2006;44(17):5174–81.
[43] Saito R, Kobayashi S, Hosoya T. J Appl Polym Sci 2005;97(5):1835–47.
[44] Saito R, Kobayashi S, Hayashi H, Shimo T. J Appl Polym Sci 2007;104(5):3388–95.
[45] Saito R, Kobayashi S, Hayashi H, Shimo T. J Appl Polym Sci 2008;109:1498–504.
[46] Gray MK, Zhou H, Nguyen ST, Torkelson JM. Macromolecules 2004;37(15):5586–95.
[47] Hata T, Nose T. J Polym Sci Part C 1967;16:2019–30.
[48] Kubo T, Tadaoka E, Kozuka H. J Sol–Gel Sci Technol 2004;31:257–61.
[49] Crank J. The mathematics of diffusion. 2nd ed. Oxford: Clarendon Press; 1975. p. 267.